crystals

MDPI

Communication

Ethoxylate Polymer-Based 96-Well Screen for Protein Crystallization

Ulrike Demmer [1], Olivier N. Lemaire [2], Mélissa Belhamri [2] and Ulrich Ermler [1,*]

[1] Max-Planck-Institute of Biophysics, Max-von-Laue-Str. 3, D-60438 Frankfurt, Germany; ulrike.demmer@biophys.mpg.de
[2] Max Planck Institute for Marine Microbiology, Celsiusstr. 1, D-28359 Bremen, Germany; olemaire@mpi-bremen.de (O.N.L.); mbelhamr@mpi-bremen.de (M.B.)
* Correspondence: ulrich.ermler@biophys.mpg.de

Abstract: Crystallization is the limiting step in X-ray structure determination of biological macromolecules. As crystallization experiments can be largely automatized, the diversity of precipitant solutions is often the determinant factor to obtain crystals of high quality. Here, we introduce a 96-well screening kit of crystallization conditions, centered on three ethoxylate-based organic polymers as precipitants and various additional compounds to promote crystal formation. This crystallization screen was tested on various non-standard proteins from bacteria and archaea. Structure determination succeeded for seven out of thirteen targets based on crystals that frequently diffracted to a higher resolution than those obtained with commercially available screening kits. Crystallization hits were rarely similar among the three ethoxylate-based organic polymers and, in comparison, with already available crystallization screens. Hence, the presented crystallization screen is an efficient tool to complement other screens and increase the likelihood of growing crystals suitable for X-ray structure determination.

Keywords: protein crystallization; crystallization screen; X-ray structure determination; glycerol ethoxylate; trimethylolpropane ethoxylate; glycerol ethoxylate-co-propoxylate triol

Citation: Demmer, U.; Lemaire, O.N.; Belhamri, M.; Ermler, U. Ethoxylate Polymer-Based 96-Well Screen for Protein Crystallization. *Crystals* **2023**, *13*, 1519. https://doi.org/10.3390/cryst13101519

Academic Editors: Vasundara Srinivasan and Santosh Panjikar

Received: 14 September 2023
Revised: 13 October 2023
Accepted: 16 October 2023
Published: 19 October 2023

1. Introduction

Although challenged by single-particle cryo-electron microscopy (cryo-EM [1]) and structure-predicting artificial intelligence approaches (Alphafold2 [2]), X-ray crystallography is still the most widely used and productive method in structural biology [3]. In particular, it is an appropriate tool for the structural characterization of protein-substrate complexes, sufficiently long-living intermediates, turnover processes in a time-resolved manner at room temperature (via X-ray free-electron laser methods), for identification and localization of metals in proteins and for high-throughput screening of a broad palette of compounds relevant for drug development due to rapid synchrotron data collection and full-automatic data processing protocols. On the other hand, X-ray crystallography suffers from different bottlenecks, the major one being the time-consuming trial-and-error process to compel a protein into a highly ordered crystalline form, which is indispensable for X-ray diffraction experiments. Together with the properties of a protein with respect to its size, purity, homogeneity, flexibility and stability, the composition of the precipitate solution is crucial for the success of crystallization. Since the first crystallization screen developed by Jancarik and Kim in 1991 [4], sophisticated screenings with a wide range of compounds have been continuously developed and are often commercially available [5–8]. The automatization of the screening process and the miniaturization of crystallization experiments using robots allow the handling of a large number of crystallization conditions, save time and protein and thereby increase the success rate. The physicochemical properties of precipitant solutions supplemented with protein are decisively governed by the central precipitant. Precipitants are usually categorized into inorganic salts, organic solvents and organic polymers. Polyethylene glycols (PEGs) are the most applied agents [9],

but alternative organic polymers are also powerful candidates [7,10–12] whose potential is not completely worked out yet. The efficiency of the precipitate solution is significantly increased using a wide range of additional agents, for example, chaotropic and kosmotropic salts, amino acids, alcohols, polyamines, sugars, detergents, reducing agents and specific bound compounds like regulators or substrates, supplemented in small amounts [13–15]. Finally, crystallization behavior is influenced by pH, which is adjusted using a buffer.

Thanks to our long-term experience, we developed a 96-well crystallization screen which is based on three soluble ethoxylate polymers as precipitants, various additives and buffers. The crystallization screen was tested on thirteen prokaryotic proteins that embody a wide range of characteristics regarding their origin, size, flexibility, purification strategies and cofactor content. Its success rate was in the range of other applied screens without indicating any apparent redundancy. The obtained crystals were of sufficient quality to determine structures without further improvement steps. In some cases, the crystals were the best diffracting specimens or even the only ones when compared with commercially available screens performed in parallel.

2. Materials and Methods

2.1. Applied Agents for Crystallization

The three polymers glycerol ethoxylate (GE 1000), trimethylolpropane ethoxylate (TMPE 1014), and glycerol ethoxylate-co-propoxylate triol (GEPT 2600) were purchased from Sigma-Aldrich GmbH. Stock solutions of 60% (*w*/*v*) were prepared with the addition of 0.1% sodium azide to prevent the growth of microorganisms, then filtered and stored frozen at −20 °C until use. 4-(2-hydroxyethyl)-1-piperazineethanesulfonic acid (HEPES), tris(hydroxymethyl)aminomethane (TRIS), ammonium sulfate ($(NH_4)_2SO_4$), potassium chloride (KCl) and glycerol were obtained from Carl Roth GmbH. Buffer solutions were prepared via adjusting the pH of 1 M stock solutions with either HCl or NaOH and subsequent filtering. Magnesium chloride ($MgCl_2$) and calcium chloride ($CaCl_2$) were bought from Merck KGaA, Darmstadt, Germany. We further purchased potassium thiocyanate (KSCN), propane-1,2-diol, L-arginine hydrochloride (L-Arg), trimethylamine-N-oxide (TMAO), D-(+)-trehalose, ectoine, sodium dithionite, dithioerythritol (DTE), adenosine diphosphate (ADP) and flavin adenine dinucleotide (FAD) from Sigma-Aldrich, St. Louis, MO, USA. 2-(N-morpholino)ethanesulfonic acid (MES) from Gerbu Biotechnik GmbH, Heidelberg, Germany, and non-detergent sulfobetaine 256 (NDSB-256) from Santa Cruz Biotechnology, Inc., Dallas, TX, USA. Adenylyl-imidodiphosphate (AMPPNP) was bought from Jena Bioscience, Jena, Germany, dithiothreitol (DTT) from Thermo Fisher Scientific, Waltham, MA, USA and L-glutamic acid (L-Glu) from Acros Organics, Geel, Belgium. The CoA-esters benzoyl-CoA and CN-benzoyl-CoA were provided by the Boll group, University of Freiburg [16] and 8-demethyl-8-amino-riboflavin-5′-phosphate (AFP) by the Mack group, University of Applied Sciences, Mannheim [17]. For all solutions, ultrapure water was used.

The commercial crystallization screens were purchased from Jena Bioscience, Jena, Germany (JBS Classic, JCSG++, JBS Pentaerythritol and PACT++), from Molecular Dimensions, Sheffield, UK (ProPlex, Morpheus I and II, Midas, Wizard Classic and Shot Gun (SG1), from Hampton Research, Aliso Viejo, CA, USA (SaltRx) and from NeXtal Biotech, Holland, MI, USA (JCSG Core Suite).

2.2. Applied Proteins

25-hydroxysteroid kinase (S25-PT) and 25-phosphosteroid lyase (S25-PSL) catalyze one reaction step each in the anaerobic sterol degradation pathway [18]. Both enzymes (Mr 43 kDa and 41 kDa) from *Sterolibacterium denitrificans* (growth temperature of 30 °C) were heterologously produced in *Escherichia coli* with a C-terminal Strep-tag. Cyclohex-1-ene-1-carboxyl-CoA dehydrogenases (CH1enDH) play a role in fermentative cyclohexane carboxylic acid degradation. The homotetrameric enzyme (Mr 164 kDa) from *Geobacter metallireducens* (growth temperature of 30 °C) was heterologously produced in *E. coli* with an N-terminal His-tag [19]. Benzoyl-CoA reductase I is involved in the aromatic degrada-

tion pathway. The heterotetrameric BCR-QONP protein complex (Mr 153 kDa) of *Thauera chlorobenzoica* 3CB-1 (growth temperature of 30 °C) was heterologously produced in *E. coli* with a C-terminal Strep-tag [20]. Phthaloyl-CoA decarboxylase (PCD) is involved in the anaerobic degradation pathway of the plastic component phthalate. The homohexameric enzyme (Mr 359 kDa) was prepared from *T. chlorobenzoica* 3CB-1 strain [21]. The double-cubane cluster protein (WP_235551353, DCCP) catalyzes the reduction of inert substrates like acetylene, but its physiological function is unknown [22]. The homodimeric enzyme (Mr 95 kDa) was isolated from *Moorella thermoacetica* DSM 521 (growth temperature of 50 °C). Carbon monoxide dehydrogenase/acetyl-CoA synthase (CODH/ACS) is involved in CO oxidation and acetogenesis. The heterotetrameric ($\alpha_2\beta_2$) enzyme (Mr 292 kDa) was directly prepared from the acetogen *Clostridium autoethanogenum* (growth temperature of 37 °C) as previously described [23]. RosC is a homodimeric enzyme (Mr 51 kDa) of roseoflavin biosynthesis. Its E107Q variant from *Streptomyces davaonensis* (growth temperature of 28 °C) was heterologously expressed in *E. coli* with an N-terminal Strep-tag [17]. Citramalate lyase (CML) is a heterotetrameric ($\alpha_2\beta_2$) enzyme (Mr 114 kDa) of the methyl aspartate pathway. It was heterologously produced from *Raoultella planticola* (growth temperature of 30 °C) with an N-terminal His-tag. Ketol-acid reductoisomerase (WP_042684866, KARI) is involved in amino acid biosynthesis and a putative target for antibiotics [24]. The dimeric (Mr 75 kDa) or dodecameric (Mr 445 kDa) enzyme (depending on the organism) was extracted from the methanogenic archaeon *Methermicoccus shengliensis* (growth temperature of 50 °C, [25]). Fructose 1,6-diphosphate aldolase (WP_042684469.1, FruA), a homodimeric enzyme (Mr 62 kDa) involved in glycolysis and gluconeogenesis [26] was also directly prepared from *M. shengliensis*. The 5,10-methylenetetrahydromethanopterin reductase (WP_042686075, Mer) and methenyltetrahydromethanopterin cyclohydrolase (WP_042685591, Mch) are homotetrameric (Mr 141 kDa) and homotrimeric (Mr 102 kDa) enzymes, respectively, applied in methanogenesis [27]. They were natively isolated from the same methanogen.

2.3. Crystallization Method and X-ray Diffraction Measurements

Crystallization was performed using the sitting-drop method with the protein and precipitant solutions listed in Table 1. Attempts under anaerobic conditions were achieved using an Oryx Nano pipetting robot (Douglas Instruments, Hungerford, UK) or manually with SWISSCI MRC 2-well plates and drop sizes of 300 + 300 or 600 + 600 nl, respectively (BCR-QONP, PCD, DCCP, CaCODH/ACS). For oxygen-insensitive proteins, crystallization screens were set up with a Phoenix Rigaku robot system using CrystalMation Intelli-plates with low profile (Art Robbins, Sunnyvale, CA, USA) and a drop size of 100 + 100 nl (RosC, S25-PSL, S25-PT, CML, CH1enDH) or manually with a drop size of 600 + 600 nl (MsKARI, MsFruA, MsMch and MsMer). Crystallization experiments were normally performed at a temperature of 18–20 °C, while for RosC, S25-PSL, S25-PT, CML and CH1enDH, additional experiments were performed at 4 °C. Obtained crystals were either frozen directly or after supplementing with a cryoprotectant. Their X-ray diffraction patterns were recorded at the Swiss-Light synchrotron source PXII (SLS, Villigen, Switzerland) and the Deutsches Elektronen-Synchrotron (DESY, Hamburg, Germany).

Table 1. Composition of the ethoxylate-based screen.

No.	Precipitant *	Buffer	Additives	No.	Precipitant *	Buffer	Additives
1	15 % TMPE 1014	0.1 M MES pH 6.5	–	49	15 % GE 1000	0.1 M Mes pH 6.5	–
2	25 % TMPE 1014	0.1 M MES pH 6.5	–	50	25 % GE 1000	0.1 M Mes pH 6.5	–
3	35 % TMPE 1014	0.1 M MES pH 6.5	–	51	35 % GE 1000	0.1 M Mes pH 6.5	–
4	45 % TMPE 1014	0.1 M MES pH 6.5	–	52	45 % GE 1000	0.1 M Mes pH 6.5	–
5	15 % TMPE 1014	0.1 M HEPES pH 7.5	–	53	15 % GE 1000	0.1 M Hepes pH 7.5	–
6	25 % TMPE 1014	0.1 M HEPES pH 7.5	–	54	25 % GE 1000	0.1 M HEPES pH 7.5	–
7	35 % TMPE 1014	0.1 M HEPES pH 7.5	–	55	35 % GE 1000	0.1 M HEPES pH 7.5	–
8	45 % TMPE 1014	0.1 M HEPES pH 7.5	–	56	45 % GE 1000	0.1 M HEPES pH 7.5	–
9	15 % TMPE 1014	0.1 M TRIS pH 8.5	–	57	15 % GE 1000	0.1 M HEPES pH 8.5	–
10	25 % TMPE 1014	0.1 M TRIS pH 8.5	–	58	25 % GE 1000	0.1 M TRIS pH 8.5	–
11	35 % TMPE 1014	0.1 M TRIS pH 8.5	–	59	35 % GE 1000	0.1 M TRIS pH 8.5	–
12	45 % TMPE 1014	0.1 M TRIS pH 8.5	–	60	45 % GE 1000	0.1 M TRIS pH 8.5	–
13	15 % TMPE 1014	0.1 M MES pH 6.5	0.05 M $MgCl_2$	61	15 % GE 1000	0.1 M MES pH 6.5	0.05 M $MgCl_2$
14	25 % TMPE 1014	0.1 M MES pH 6.5	0.1 M $CaCl_2$	62	25 % GE 1000	0.1 M MES pH 6.5	0.1 M $CaCl_2$
15	35 % TMPE 1014	0.1 M MES pH 6.5	0.2 M $(NH_4)_2SO_4$	63	35 % GE 1000	0.1 M MES pH 6.5	0.2 M $(NH_4)_2SO_4$
16	45 % TMPE 1014	0.1 M MES pH 6.5	0.4 M KCl	64	45 % GE 1000	0.1 M MES pH 6.5	0.4 M KCl
17	15 % TMPE 1014	0.1 M HEPES pH 7.5	0.05 M $MgCl_2$	65	15 % GE 1000	0.1 M HEPES pH 7.5	0.05 M $MgCl_2$
18	25 % TMPE 1014	0.1 M HEPES pH 7.5	0.1 M $CaCl_2$	66	25 % GE 1000	0.1 M HEPES pH 7.5	0.1 M $CaCl_2$
19	35 % TMPE 1014	0.1 M HEPES pH 7.5	0.2 M $(NH_4)_2SO_4$	67	35 % GE 1000	0.1 M HEPES pH 7.5	0.2 M $(NH_4)_2SO_4$
20	45 % TMPE 1014	0.1 M HEPES pH 7.5	0.4 M KCl	68	45 % GE 1000	0.1 M HEPES pH 7.5	0.4 M KCl
21	15 % TMPE 1014	0.1 M TRIS pH 8.5	0.05 M $MgCl_2$	69	15 % GE 1000	0.1 M TRIS pH 8.5	0.05 M $MgCl_2$
22	25 % TMPE 1014	0.1 M TRIS pH 8.5	0.1 M $CaCl_2$	70	25 % GE 1000	0.1 M TRIS pH 8.5	0.1 M $CaCl_2$
23	35 % TMPE 1014	0.1 M TRIS pH 8.5	0.2 M $(NH_4)_2SO_4$	71	35 % GE 1000	0.1 M TRIS pH 8.5	0.2 M $(NH_4)_2SO_4$
24	45 % TMPE 1014	0.1 M TRIS pH 8.5	0.4 M KCl	72	45 % GE 1000	0.1 M TRIS pH 8.5	0.4 M KCl
25	15 % TMPE 1014	0.1 M MES pH 6.5	10 % (*v*/*v*) Propane-1,2-diol	73	15 % GEPT 2600	0.1 M MES pH 6.5	–
26	25 % TMPE 1014	0.1 M MES pH 6.5	0.2 M KSCN	74	25 % GEPT 2600	0.1 M MES pH 6.5	–
27	35 % TMPE 1014	0.1 M MES pH 6.5	5 % Glycerol	75	35 % GEPT 2600	0.1 M MES pH 6.5	–
28	45 % TMPE 1014	0.1 M MES pH 6.5	50 mM L-Arg, 50 mM L-Glu	76	45 % GEPT 2600	0.1 M MES pH 6.5	–
29	15 % TMPE 1014	0.1 M HEPES pH 7.5	10 % (*v*/*v*) Propane-1,2-diol	77	15 % GEPT 2600	0.1 M HEPES pH 7.5	–
30	25 % TMPE 1014	0.1 M HEPES pH 7.5	0.2 M KSCN	78	25 % GEPT 2600	0.1 M HEPES pH 7.5	–
31	35 % TMPE 1014	0.1 M HEPES pH 7.5	5 % Glycerol	79	35 % GEPT 2600	0.1 M HEPES pH 7.5	–
32	45 % TMPE 1014	0.1 M HEPES pH 7.5	50 mM L-Arg, 50 mM L-Glu	80	45 % GEPT 2600	0.1 M HEPES pH 7.5	–
33	15 % TMPE 1014	0.1 M TRIS pH 8.5	10 % (*v*/*v*) Propane-1,2-diol	81	15 % GEPT 2600	0.1 M TRIS pH 8.5	–
34	25 % TMPE 1014	0.1 M TRIS pH 8.5	0.2 M KSCN	82	25 % GEPT 2600	0.1 M TRIS pH 8.5	–
35	35 % TMPE 1014	0.1 M TRIS pH 8.5	5 % Glycerol	83	35 % GEPT 2600	0.1 M TRIS pH 8.5	–
36	45 % TMPE 1014	0.1 M TRIS pH 8.5	50 mM L-Arg, 50 mM L-Glu	84	45 % GEPT 2600	0.1 M TRIS pH 8.5	–
37	15 % TMPE 1014	0.1 M MES pH 6.5	0.2 M TMAO	85	15 % GEPT 2600	0.1 M MES pH 6.5	0.05 M $MgCl_2$
38	25 % TMPE 1014	0.1 M MES pH 6.5	0.4 M D-(+)-Trehalose	86	25 % GEPT 2600	0.1 M MES pH 6.5	0.1 M $CaCl_2$
39	35 % TMPE 1014	0.1 M MES pH 6.5	0.25 M Ectoine	87	35 % GEPT 2600	0.1 M MES pH 6.5	0.2 M $(NH_4)_2SO_4$
40	45 % TMPE 1014	0.1 M MES pH 6.5	0.15 M NDSB-256	88	45 % GEPT 2600	0.1 M MES pH 6.5	0.4 M KCl
41	15 % TMPE 1014	0.1 M HEPES pH 7.5	0.2 M TMAO	89	15 % GEPT 2600	0.1 M HEPES pH 7.5	0.05 M $MgCl_2$
42	25 % TMPE 1014	0.1 M HEEPS pH 7.5	0.4 M D-(+)-Trehalose	90	25 % GEPT 2600	0.1 M HEPES pH 7.5	0.1 M $CaCl_2$
43	35 % TMPE 1014	0.1 M HEPES pH 7.5	0.25 M Ectoine	91	35 % GEPT 2600	0.1 M HEPES pH 7.5	0.2 M $(NH_4)_2SO_4$
44	45 % TMPE 1014	0.1 M HEPES pH 7.5	0.15 M NDSB-256	92	45 % GEPT 2600	0.1 M HEPES pH 7.5	0.4 M KCl
45	15 % TMPE 1014	0.1 M TRIS pH 8.5	0.2 M TMAO	93	15 % GEPT 2600	0.1 M TRIS pH 8.5	0.05 M $MgCl_2$
46	25 % TMPE 1014	0.1 M TRIS pH 8.5	0.4 M D-(+)-Trehalose	94	25 % GEPT 2600	0.1 M TRIS pH 8.5	0.1 M $CaCl_2$
47	35 % TMPE 1014	0.1 M TRIS pH 8.5	0.25 M Ectoine	95	35 % GEPT 2600	0.1 M TRIS pH 8.5	0.2 M $(NH_4)_2SO_4$
48	45 % TMPE 1014	0.1 M TRIS pH 8.5	0.15 M NDSB-256	96	45 % GEPT 2600	0.1 M TRIS pH 8.5	0.4 M KCl

* All percentages are given as weight per volume (*w*/*v*), except for those indicated.

3. Results and Discussion

3.1. The Composition of the Crystallization Screen

Organic polymers have proven to be valuable precipitants for protein crystallization [7,10–12]. They reduce the protein solubility through modifying the local ionic strength [28], decreasing the masking of proteins and/or neutralizing their charges. The interactions between a protein and its surrounding bulk solvent environment are lowered [13,29], and the magnitude of hydrophobic and hydrogen-bond forces among protein molecules is enhanced. In addition, the altered viscosity influences the kinetics of crystal growth. Preliminary experiments involving lysozyme as the test object pointed toward the organic polymers glycerol ethoxylate (GE 1000), trimethylolpropane ethoxylate (TMPE 1014) and glycerol ethoxylate-co-propoxylate triol (GEPT 2600) (Figure 1) as promising precipitants, which became the major components of the 96-well screening kit (Table 1). Trimethylolpropane ethoxylates with lower molecular masses, such as TMPE 170 and TMPE 450, were also tested for their use as precipitants, but they turned out to be less efficient.

As additional chemical compounds, we used different salts ($MgCl_2$, $CaCl_2$, KCl, $(NH_4)_2SO_4$ and KSCN) that are well established to support crystal formation [30], as well as a set of small molecules chosen because of their favorable influence on protein stability and crystal nucleation. The cryoprotectant glycerol was used for its role in stabilizing proteins, suppressing their flexibility and aggregation and reducing their nucleation rate [31–33]. The additive propane-1,2-diol is used as a stabilizer [34] and cryoprotectant in cryo-crystallography as an alternative to glycerol or ethylene glycol [35,36]. L-Glu and L-Arg (50 mM each) had a synergistic effect on the solubility of the tested proteins [37], and L-Arg was found to prevent aggregation and increase protein stability [38,39]. The disaccharide trehalose (Figure 1) was reported to enhance the nucleation of both lysozyme and thaumatin [40]. The osmolyte trimethylamine N-oxide (TMAO, Figure 1) protects intracellular components against osmotic stress and hydrostatic pressure [41] and increases the stability and nucleation properties of proteins [42]. The amino acid 2-methyl-14,5,6-tetrahydropyrimidine-4-carboxylic acid (ectoine, Figure 1) [43] protects proteins from stress factors like heat, freezing, drying or mechanical forces [44], suppresses aggregation [45] and might increase the crystal size [46]. Finally, NDSB-256 (Figure 1), a non-detergent zwitterionic sulfobetaine, stabilizes proteins, reduces their aggregation and favors the growth of ordered crystals [47,48].

Three buffers at different pH (MES buffer pH 6.5, HEPES buffer pH 7.5 and TRIS buffer pH 8.5) were the final variables of the crystallization screen (Table 1). The pH measurements of the entire crystallization solution indicated ΔpH deviations from the buffer pH of up to 0.2 for GE 1000 and GEPT 2600 as well as about 0.5 for TMPE 1014. Precipitants, additives and buffers were mixed in a matrix of 96 different crystallization conditions, which were tested on different non-standard proteins to determine their practical suitability.

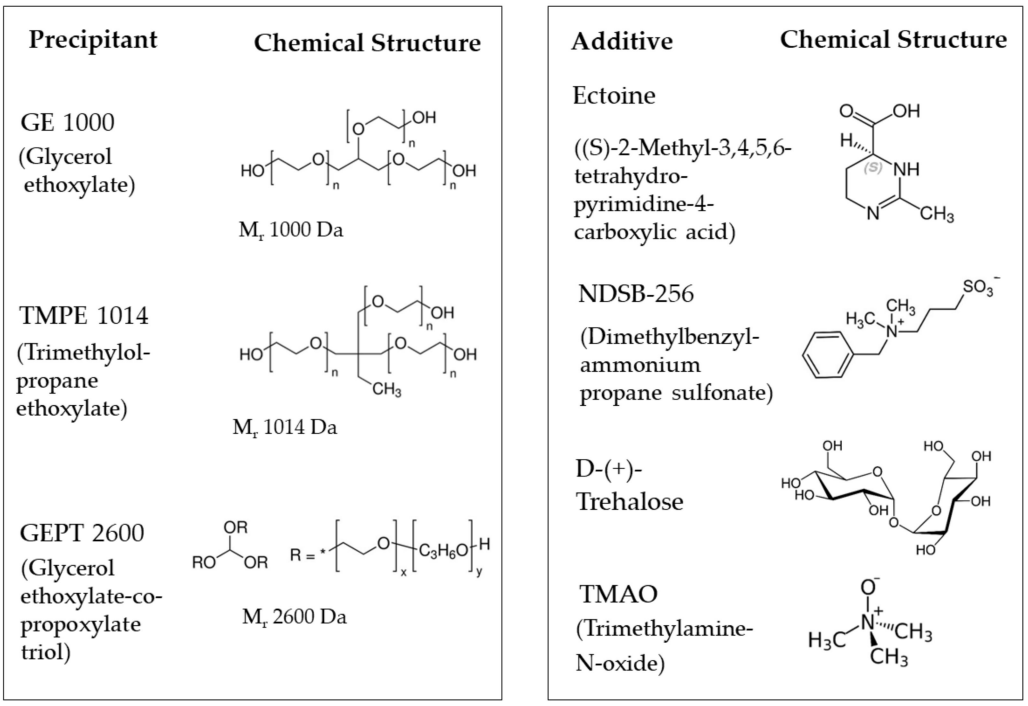

Figure 1. Chemical structures of the precipitants and some additives.

3.2. Application to Proteins

The quality of the ethoxylate-derived screening kit was assessed using a set of thirteen proteins with a wide range of different properties. The protein targets varied in size between 25 and 445 kDa with oligomeric state between dimers and dodecamers. They were natively extracted or heterologously expressed from mesophilic and thermophilic organisms belonging to archaea and bacteria. Some targets contained only the polypeptide, while others contained additional cofactors and individual substrates. Purification and crystallization were attempted under aerobic or anaerobic conditions. The success rate of the thirteen proteins applied was in the range found for the PACT++ and JBS pentaerythritol screens, tested for nine and eight proteins. A summary of each project is given in Table 2. For seven of the tested proteins (BCR-QONP, CODH/ACS, DCCP, S25-PT, RosC-E107Q, MsFruA and MsMch), the crystal quality was sufficient for structure determination (Figure 2, Table 2). For some projects, the crystals from the ethoxylate-based screening kit diffracted to the highest resolution. For one project (S25-PT), only the ethoxylate-based screening kit produced suitable X-ray crystals (Table 2). Furthermore, the overall efficiency may have been underestimated, as optimization was stopped when any of the applied kits provided high-quality crystals of the desired protein or protein state. Altogether, crystallization of the thirteen proteins succeeded at least once in sixty-three out of the ninety-six conditions. The three precipitants provided suitable crystallization conditions in comparable amounts and rarely yielded identical hits under the same buffer and additive conditions. Crystal vitrification for data collection is usually straightforward, as their concentrations have to be increased to 45%–50%, further underscoring the utility of the three precipitants. An analysis of the impact of every additive for successful crystallization puts the salts and the L-Glu/L-Arg mixture at the top. According to limited statistics, the number of crystallization hits is significantly higher at pH values of 6.5 or 8.5 than at neutral pH, which perhaps reflects the extremophilic origin of some of the tested proteins and their accompanying protein stability and rigidity at non-neutral pH values. The statistically most successful solution was, however, obtained at a near-neutral pH with a composition of 35% GEPT 2600, 0.1 M HEPES, pH 7.5 and 0.2 M $(NH_4)_2SO_4$, resulting in five hits. For the applied proteins, the propensity to crystallize did not appear to be influenced by size but rather by the optimal growth temperature of the host organism (Table 2). The crystallization rate of

proteins that originate from thermophilic organisms (*M. thermoacetica* and *M. shengliensis*, optimal growth temperatures of 50 °C) is higher than that from mesophilic species (Table 2). However, it is worth mentioning that a larger fraction of the thermophilic proteins is prepared from natural sources and not through heterologous expression. The impact of this factor on crystallization has not yet been explored.

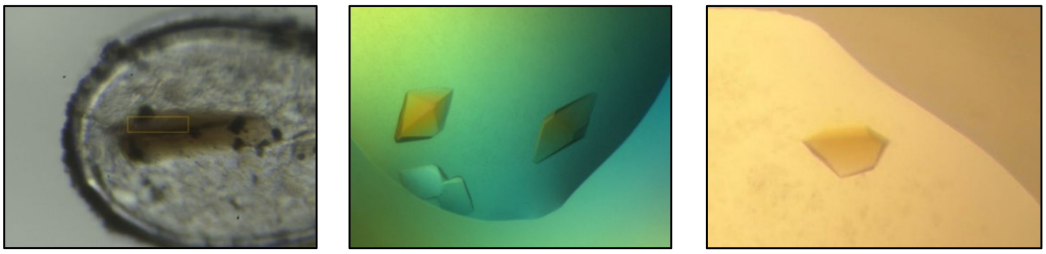

(**a**) (**b**) (**c**)

Figure 2. Best diffracting crystals for three proteins grown with the ethoxylate polymer-based screen. (**a**) DCCP (1.6 Å), (**b**) S-25-PT (2.1 Å), (**c**) BCR-QONP (2.5 Å).

Our results again demonstrate the importance of using multiple crystallization screens. The newly developed ethoxylate-derived screen (Table 1) exhibited a high crystallization success rate and resulted in many crystals with good diffraction, which allowed the structure determination of several non-standard and never-characterized proteins. The ethoxylate-based screening kit is approximately as beneficial as other established commercial screening kits without apparent overlap. It is therefore a suitable tool to complement other kits to maximize the crystallization success of proteins, thereby indicating that the search for new precipitants for crystallization is still possible and worthwhile.

Table 2. Results of the tested proteins (x: few crystals, xx: several crystals, xxx: many crystals).

Protein	**BCR-QONP**		**Ch1-2en-DH**		**CML**		**CODH/ACS**		**DCCP**		**MsKARI**		**MsFruA**	
Added ligands	5 mM Benzoyl-CoA 5 mM ADP 5 mM $MgCl_2$		0.1 mM FAD		5 mM AMPPNP		–		–		–		–	
Most successful ethoxylate precipitant	GE 1000						GE 1000		GEPT 2600		TMPE 1014		TMPE 1014	
	Screens used	Hits/best resolution/ precipitant	Screens used	Hits/best resolution/ precipitant	Screens used	Hits/best resolution/ precipitant	Screens used	Hits/best resolution/ precipitant	Screens used	Hits/best resolution/ precipitant	Screens used	Hits/best resolution/ precipitant	Screens used	Hits/best resolution/ precipitant
Ethoxylate based screen	•	xx/2.5 Å (GE 1000)	•		•		•	xx/2.9 Å (GE 1000)	•	xxx/1.6 Å (GEPT 2600)	•	xx	•	xxx/2.0Å (TMPE 1014)
JCSG++							•	x			•	xx/2.9 Å $(NH_4)_2SO_4$		
JCSG Core Suite I			•	x/2.1 Å (PEG 3350)										
JBS Classic 1-4	•	x	•	x	•	x/3.0 Å (PEG 4000)								
JBS Classic 5-8	•	–	•	xx	•	x								
Midas	•	x												
Morpheus I	•	x	•	–	•	–								
Morpheus II	•	x	•	x	•	–								
PACT++	•	–	•	x	•	–					•	xxx	•	xxx
JBS Pentaerythritol	•	x	•	x	•	xx							•	xx
ProPlex	•	–					•	x						
SaltRx			•	–										
SG1							•	xxx					•	xxx/1.9 Å (PEG 3350)
Wizard Classic 1							•	–			•	x		
Wizard Classic 2							•	x			•	x		
Wizard Classic 3							•	x			•	xx		
Wizard Classic 4							•	x			•	xx		

Table 2. *Cont.*

Protein	**MsMch**		**MsMer**		**PCD**		**RosC-E107Q**		**25-PSL**		**S25-PT**	
Added ligands	–		–		5 mM CN-benzoyl-CoA		5 mM AFP		–		5 mM ADP	
Most successful ethoxylate precipitant	TMPE 1014		GEPT 2600		GE 1000		GE 1000		TMPE 1014		TMPE 1014	
	Screens used	Hits/best resolution/ precipitant	Screens used	Hits/best resolution/ precipitant	Screens used	Hits/best resolution/ precipitant	Screens used	Hits/best resolution/ precipitant	Screens used	Hits/best resolution/ precipitant	Screens used	Hits/best resolution/ precipitant
Ethoxylate based screen	•	xx/2.7 Å (TMPE 1014)	•	xxx	•	x	•	xx/3.5 Å (GE 1000)	•	x	•	xx/2.1 Å (TMPE 1014)
JCSG++			•	xx/2.2 Å (PEG 3350)								
JCSG Core Suite I												
JBS Classic 1-4					•	x	•	x	•	x	•	x
JBS Classic 5-8							•	x	•	x/3.0 Å (PEG 8000)	•	–
Midas												
Morpheus I					•	xx/2.0 Å (PEG 8000)	•	xx				
Morpheus II					•	xx	•	x				
PACT++					•	x	•	x/2.9 Å (PEG 3350)	•	xxx	•	–
JBS Pentaerythritol					•	x	•	x	•	x	•	–
ProPlex												
SaltRx									•	x	•	–
SG1	•	xx/2.0 Å (PEG 3350)	•	xx								
Wizard Classic 1												
Wizard Classic 2												
Wizard Classic 3												
Wizard Classic 4												

Author Contributions: Conceptualization, U.D. and U.E.; methodology, validation, formal analysis, investigation, resources, data curation, U.D., M.B., O.N.L. and U.E.; writing—original draft preparation, U.D. and U.E.; writing—review and editing, U.D., M.B., O.N.L. and U.E.; visualization, U.D.; supervision, U.E.; project administration, U.D. All authors have read and agreed to the published version of the manuscript.

Funding: This research received no external funding.

Data Availability Statement: Further information about this work can be obtained upon request.

Acknowledgments: We thank Hartmut Michel and Tristan Wagner for their continuous support. We are grateful to Jonathan Fuchs, Christian Jacoby, Robin Geiger, Johannes Kung, Matthias Boll, Jessica Eggers, Ivan Berg, Tanya Joshi and Matthias Mack for providing proteins. We further thank Barbara Rathmann for long-term support in setting up crystallization screens, the Max Planck Society and the staff of both the SLS and DESY synchrotrons for their work and help.

Conflicts of Interest: The authors declare no conflict of interest.

References

1. Kühlbrandt, W. Biochemistry. The resolution revolution. *Science* **2014**, *343*, 1443–1444. [CrossRef] [PubMed]
2. Jumper, J.; Evans, R.; Pritzel, A.; Green, T.; Figurnov, M.; Ronneberger, O.; Tunyasuvunakool, K.; Bates, R.; Zidek, A.; Potapenko, A.; et al. Highly accurate protein structure prediction with AlphaFold. *Nature* **2021**, *596*, 583–589. [CrossRef] [PubMed]
3. Gorrec, F. A beginner's guide to macromolecular crystallization. *Biochemist* **2021**, *43*, 36–43. [CrossRef]
4. Jancarik, J.; Kim, S.H. Sparse-Matrix Sampling—A Screening Method for Crystallization of Proteins. *J. Appl. Crystallogr.* **1991**, *24*, 409–411. [CrossRef]
5. Gorrec, F. The MORPHEUS protein crystallization screen. *J. Appl. Crystallogr.* **2009**, *42*, 1035–1042. [CrossRef] [PubMed]
6. Newman, J.; Egan, D.; Walter, T.S.; Meged, R.; Berry, I.; Ben Jelloul, M.; Sussman, J.L.; Stuart, D.I.; Perrakis, A. Towards rationalization of crystallization screening for small- to medium-sized academic laboratories: The PACT/JCSG+ strategy. *Acta Crystallogr. D Biol. Crystallogr.* **2005**, *61*, 1426–1431. [CrossRef]
7. Grimm, C.; Chari, A.; Reuter, K.; Fischer, U. A crystallization screen based on alternative polymeric precipitants. *Acta Crystallogr. D Biol. Crystallogr.* **2010**, *66*, 685–697. [CrossRef] [PubMed]
8. Gorrec, F. The MORPHEUS II protein crystallization screen. *Acta Crystallogr. F Struct. Biol. Commun.* **2015**, *71*, 831–837. [CrossRef] [PubMed]
9. McPherson, A., Jr. Crystallization of proteins from polyethylene glycol. *J. Biol. Chem.* **1976**, *251*, 6300–6303. [CrossRef] [PubMed]
10. Patel, S.; Cudney, B.; McPherson, A. Polymeric precipitants for the crystallization of macromolecules. *Biochem. Biophys. Res. Commun.* **1995**, *207*, 819–828. [CrossRef] [PubMed]
11. Skalova, T.; Duskova, J.; Hasek, J.; Kolenko, P.; Stepankova, A.; Dohnalek, J. Alternative polymer precipitants for protein crystallization. *J. Appl. Crystallogr.* **2010**, *43*, 737–742. [CrossRef]
12. Gulick, A.M.; Horswill, A.R.; Thoden, J.B.; Escalante-Semerena, J.C.; Rayment, I. Pentaerythritol propoxylate: A new crystallization agent and cryoprotectant induces crystal growth of 2-methylcitrate dehydratase. *Acta Crystallogr. D Biol. Crystallogr.* **2002**, *58*, 306–309. [CrossRef] [PubMed]
13. McPherson, A.; Cudney, B. Searching for silver bullets: An alternative strategy for crystallizing macromolecules. *J. Struct. Biol.* **2006**, *156*, 387–406. [CrossRef] [PubMed]
14. Kaushik, J.K.; Bhat, R. Why Is Trehalose an Exceptional Protein Stabilizer?: An analysis of the thermal stability of proteins in the presence of the compatible osmolyte trehalose. *J. Biol. Chem.* **2003**, *278*, 26458–26465. [CrossRef]
15. Sauter, C.; Ng, J.D.; Lorber, B.; Keith, G.; Brion, P.; Hosseini, M.W.; Lehn, J.M.; Giege, R. Additives for the crystallization of proteins and nucleic acids. *J. Cryst. Growth* **1999**, *196*, 365–376. [CrossRef]
16. Willistein, M.; Haas, J.; Fuchs, J.; Estelmann, S.; Ferlaino, S.; Müller, M.; Ludeke, S.; Boll, M. Enantioselective Enzymatic Naphthoyl Ring Reduction. *Chem.-Eur. J.* **2018**, *24*, 12505–12508. [CrossRef]
17. Schneider, C.; Konjik, V.; Kissling, L.; Mack, M. The novel phosphatase RosC catalyzes the last unknown step of roseoflavin biosynthesis in *Streptomyces davaonensis*. *Mol. Microbiol.* **2020**, *114*, 609–625. [CrossRef] [PubMed]
18. Jacoby, C.; Goerke, M.; Bezold, D.; Jessen, H.; Boll, M. A fully reversible 25-hydroxy steroid kinase involved in oxygen-independent cholesterol side-chain oxidation. *J. Biol. Chem.* **2021**, *297*, 101105. [CrossRef] [PubMed]
19. Kung, J.W.; Meier, A.K.; Willistein, M.; Weidenweber, S.; Demmer, U.; Ermler, U.; Boll, M. Structural Basis of Cyclic 1,3-Diene Forming Acyl-Coenzyme A Dehydrogenases. *Chembiochem* **2021**, *22*, 3173–3177. [CrossRef]
20. Tiedt, O.; Fuchs, J.; Eisenreich, W.; Boll, M. A catalytically versatile benzoyl-CoA reductase, key enzyme in the degradation of methyl- and halobenzoates in denitrifying bacteria. *J. Biol. Chem.* **2018**, *293*, 10264–10274. [CrossRef]
21. Mergelsberg, M.; Willistein, M.; Meyer, H.; Stark, H.J.; Bechtel, D.F.; Pierik, A.J.; Boll, M. Phthaloyl-coenzyme A decarboxylase from Thauera chlorobenzoica: The prenylated flavin-, K^+- and Fe^{2+}-dependent key enzyme of anaerobic phthalate degradation. *Environ. Microbiol.* **2017**, *19*, 3734–3744. [CrossRef] [PubMed]

22. Jeoung, J.H.; Nicklisch, S.; Dobbek, H. Structural basis for coupled ATP-driven electron transfer in the double-cubane cluster protein. *Proc. Natl. Acad. Sci. USA* **2022**, *119*, e2203576119. [CrossRef] [PubMed]
23. Lemaire, O.N.; Wagner, T. Gas channel rerouting in a primordial enzyme: Structural insights of the carbon-monoxide dehydrogenase/acetyl-CoA synthase complex from the acetogen *Clostridium autoethanogenum*. *BBA-Bioenerg.* **2021**, *1862*, 148330. [CrossRef] [PubMed]
24. Lemaire, O.N.; Müller, M.C.; Kahnt, J.; Wagner, T. Structural Rearrangements of a Dodecameric Ketol-Acid Reductoisomerase Isolated from a Marine Thermophilic Methanogen. *Biomolecules* **2021**, *11*, 1679. [CrossRef] [PubMed]
25. Cheng, L.; Qiu, T.L.; Yin, X.B.; Wu, X.L.; Hu, G.Q.; Deng, Y.; Zhang, H. *Methermicoccus shengliensis* gen. nov., sp nov., a thermophilic, methylotrophic methanogen isolated from oil-production water, and proposal of Methermicoccaceae fam. nov. *Int. J. Syst. Evol. Micr.* **2007**, *57*, 2964–2969. [CrossRef] [PubMed]
26. Izard, T.; Sygusch, J. Induced fit movements and metal cofactor selectivity of class II aldolases—Structure of thermus aquaticus fructose-1,6-bisphosphate aldolase. *J. Biol. Chem.* **2004**, *279*, 11825–11833. [CrossRef]
27. Grabarse, W.; Vaupel, M.; Vorholt, J.A.; Shima, S.; Thauer, R.K.; Wittershagen, A.; Bourenkov, G.; Bartunik, H.D.; Ermler, U. The crystal structure of methenyltetrahydromethanopterin cyclohydrolase from the hyperthermophilic archaeon *Methanopyrus kandleri*. *Structure* **1999**, *7*, 1257–1268. [CrossRef] [PubMed]
28. Song, R.Q.; Colfen, H. Additive controlled crystallization. *Crystengcomm* **2011**, *13*, 1249–1276. [CrossRef]
29. McPherson, A.; Nguyen, C.; Cudney, R.; Larson, S.B. The Role of Small Molecule Additives and Chemical Modification in Protein Crystallization. *Cryst. Growth Des.* **2011**, *11*, 1469–1474. [CrossRef]
30. Trakhanov, S.; Quiocho, F.A. Influence of Divalent-Cations in Protein Crystallization. *Protein Sci.* **1995**, *4*, 1914–1919. [CrossRef]
31. Sousa, R. Use of Glycerol, Polyols and Other Protein-Structure Stabilizing Agents in Protein Crystallization. *Acta Crystallogr. D* **1995**, *51*, 271–277. [CrossRef] [PubMed]
32. Vagenende, V.; Yap, M.G.; Trout, B.L. Mechanisms of protein stabilization and prevention of protein aggregation by glycerol. *Biochemistry* **2009**, *48*, 11084–11096. [CrossRef]
33. Vera, L.; Czarny, B.; Georgiadis, D.; Dive, V.; Stura, E.A. Practical Use of Glycerol in Protein Crystallization. *Cryst. Growth Des.* **2011**, *11*, 2755–2762. [CrossRef]
34. Singh, S.; Singh, J. Effects of polyols on the conformational stability and biological activity of a model protein lysozyme. *AAPS PharmSciTech* **2003**, *4*, E42. [CrossRef] [PubMed]
35. Douzou, P. Aqueous-organic solutions of enzymes at sub-zero temperatures. *Biochimie* **1971**, *53*, 1135–1145. [CrossRef]
36. Sankha, B. Cryoprotectants and Their Usage in Cryopreservation Process. In *Cryopreservation Biotechnology in Biomedical and Biological Sciences*; Yusuf, B., Ed.; IntechOpen: Rijeka, Croatia, 2018; Chapter 2; pp. 7–19. [CrossRef]
37. Golovanov, A.P.; Hautbergue, G.M.; Wilson, S.A.; Lian, L.Y. A simple method for improving protein solubility and long-term stability. *J. Am. Chem. Soc.* **2004**, *126*, 8933–8939. [CrossRef] [PubMed]
38. Shaikh, A.R.; Shah, D. Arginine-Amino Acid Interactions and Implications to Protein Solubility and Aggregation. *J. Eng. Res. TJER* **2015**, *12*, 1–14. [CrossRef]
39. Arakawa, T.; Ejima, D.; Tsumoto, K.; Obeyama, N.; Tanaka, Y.; Kita, Y.; Timasheff, S.N. Suppression of protein interactions by arginine: A proposed mechanism of the arginine effects. *Biophys. Chem.* **2007**, *127*, 1–8. [CrossRef]
40. Yancey, P.H. Organic osmolytes as compatible, metabolic and counteracting cytoprotectants in high osmolarity and other stresses. *J. Exp. Biol.* **2005**, *208*, 2819–2830. [CrossRef]
41. Yancey, P.H.; Gerringer, M.E.; Drazen, J.C.; Rowden, A.A.; Jamieson, A. Marine fish may be biochemically constrained from inhabiting the deepest ocean depths. *Proc. Natl. Acad. Sci. USA* **2014**, *111*, 4461–4465. [CrossRef] [PubMed]
42. Russo, A.T.; Rösgen, J.; Bolen, D.W. Osmolyte Effects on Kinetics of FKBP12 C22A Folding Coupled with Prolyl Isomerization. *J. Mol. Biol.* **2003**, *330*, 851–866. [CrossRef] [PubMed]
43. Galinski, E.A.; Pfeiffer, H.P.; Trüper, H.G. 1,4,5,6-Tetrahydro-2-methyl-4-pyrimidinecarboxylic acid. A novel cyclic amino acid from halophilic phototrophic bacteria of the genus Ectothiorhodospira. *Eur. J. Biochem.* **1985**, *149*, 135–139. [CrossRef] [PubMed]
44. Lippert, K.; Galinski, E.A. Enzyme stabilization be ectoine-type compatible solutes: Protection against heating, freezing and drying. *Appl. Microbiol. Biotechnol.* **1992**, *37*, 61–65. [CrossRef]
45. Salmannejad, F.; Nafissi-Varcheh, N. Ectoine and hydroxyectoine inhibit thermal-induced aggregation and increase thermostability of recombinant human interferon Alfa2b. *Eur. J. Pharm. Sci.* **2017**, *97*, 200–207. [CrossRef] [PubMed]
46. Harjes, S.; Scheidig, A.; Bayer, P. Expression, purification and crystallization of human 3′-phosphoadenosine-5′-phosphosulfate synthetase 1. *Acta Crystallogr. D Biol. Crystallogr.* **2004**, *60*, 350–352. [CrossRef]
47. Expert-Bezancon, N.; Rabilloud, T.; Vuillard, L.; Goldberg, M.E. Physical-chemical features of non-detergent sulfobetaines active as protein-folding helpers. *Biophys. Chem.* **2003**, *100*, 469–479. [CrossRef]
48. Vuillard, L.; Baalbaki, B.; Lehmann, M.; Norager, S.; Legrand, P.; Roth, M. Protein crystallography with non-detergent sulfobetaines. *J. Cryst. Growth* **1996**, *168*, 150–154. [CrossRef]